Far-infrared and near-millimeter spectroscopy of the $Rb_{0.5}(NH_4)_{0.5}H_2PO_4$ dipolar glass

1991 J. Phys.: Condens. Matter 3 2021

(http://iopscience.iop.org/0953-8984/3/13/005)

J. Phys.: Condens. Matter 3 (1991) 2021–2027. Printed in the UK

Far-infrared and near-millimetre spectroscopy of the $Rb_{0.5}(NH_4)_{0.5}H_2PO_4$ dipolar glass

J Petzelt†, V Železný†, S Kamba†, A V Sinitski‡, S P Lebedev‡, A A Volkov‡, G V Kozlov‡ and V H Schmidt§

† Institute of Physics, Czechoslovak Academy of Sciences, Na Slovance 2, 18040 Prague 8, Czechoslovakia

‡ Institute of General Physics, Academy of Sciences of the USSR, Vavilov Street 38, 177 333 Moscow, USSR

§ Department of Physics, Montana State University, Bozeman, MT 59717, USA

Received 30 August 1990

Abstract. The dielectric response of the $Rb_{0.5}(NH_4)_{0.5}H_2PO_4$ dipolar glass was determined in the spectral range 8–650 cm^{-1} and temperature range 10–300 K using BWO monochromatic transmission spectroscopy (8–18 cm^{-1}) and Fourier transform reflection spectroscopy (20–650 cm^{-1}). Above the glass transition temperature $T_g = 100$ K the low-frequency dynamics (below about 100 cm^{-1}) is similar to that of an averaged pure crystal. The observed one- and two-mode behaviour in the phonon region confirms the earlier Raman results. Below T_g a broad background absorption in addition to phonon peaks remain present down to the lowest temperatures especially for the $E \perp c$ polarization. We suggest that this is caused by breaking of the quasi-momentum conservation selection rule. The appearance of new forbidden modes below T_g gives evidence of polar microregions. The low-frequency dispersion below T_g is caused by different collective proton-hopping process from the higher-frequency soft-mode-type hopping, probably because of specific diffusion of Takagi defects.

1. Introduction

Despite the large effort devoted to the study of magnetic spin and electric dipolar glasses during the last decade (see the review by Binder and Young (1986)), many questions remain still open. Of the dipolar glasses the ferroelectric–antiferroelectric solid solution $Rb_{1-x}(NH_4)_xH_2PO_4$ (RADP) is the best and most intensively investigated system, especially concerning its dynamical properties (Courtens 1987). The system shows a sharp ferroelectric transition for $x < 0.22$ and an antiferroelectric transition for $x > 0.74$ and forms a dipolar glass below $T_g \simeq 100$ K for the intermediate values of x (Courtens 1987). Thorough audiofrequency (Courtens 1984, 1986) and microwave (Brückner *et al* 1988) dielectric measurements, polarization saturation experiments (Courtens and Vogt 1986), Raman spectroscopy (Courtens and Vogt 1985, 1986) and Brillouin spectroscopy (Courtens *et al* 1985, 1986, Courtens and Vacher 1987) have been carried out on this system especially for $x = 0.35$. They revealed extremely broad absorption and dispersion processes in the glassy phase. The only infrared data known to the present authors are obtained with powder samples (Le Calve *et al* 1989). Therefore the dielectric dispersion

0953-8984/91/132021 + 07 $03.50

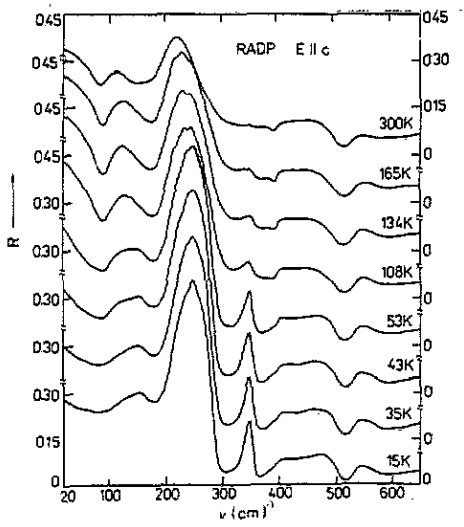

Figure 1. Temperature dependence of the RADP reflectivity spectra for $E \| c$ polarization (B_2 modes).

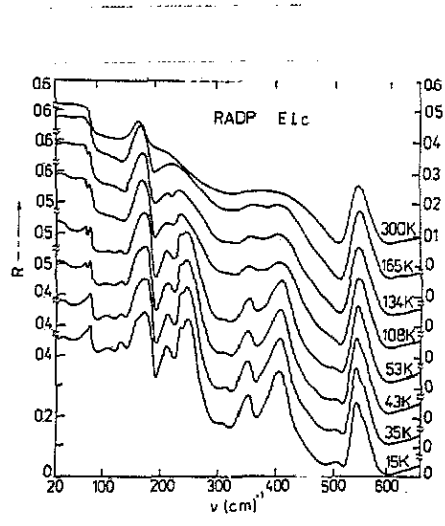

Figure 2. As for figure 1 but for $E \perp c$ polarization (E modes).

above 10^{10} Hz remains still unknown. In this paper we report far-infrared and near-millimetre measurements with single crystals for $x = 0.5$ which try to fill in this gap in the experimental studies of the RADP system.

2. Experimental details

Polarized reflectivity spectra in the range 20–650 cm^{-1} and at a temperature 15–300 K were measured using a Bruker IFS 113v Fourier spectrometer. The sample was a polished a-plate of about 0.3 cm^2 area and about 1 mm thickness. Polarised transmission measurements in the range 8–18 cm^{-1} and temperature 5–300 K were performed with the home-made tunable monochromatic backward-wave-oscillator spectrometer Epsilon (Volkov *et al* 1985). The sample was a plane-parallel a-plate of about 0.3 cm^2 area and 0.155 mm thickness. In this spectrometer both the phase of the transmitted wave and the power transmission are measured simultaneously so that the complex dielectric spectra can be calculated directly.

3. Results and evaluation

In figures 1 and 2 we show the temperature dependence of the reflectivity spectra for polarization $E \| c$ (B_2 modes) and $E \perp c$ (E modes), respectively. The spectra were normalized to merge into the more accurate values calculated from the transmission measurements at the low-frequency end. The normalized spectra were evaluated by Kramers–Kronig analysis to calculate the phase of the reflected wave and the complex dielectric function. Outside the measured spectral range the reflectivity was assumed

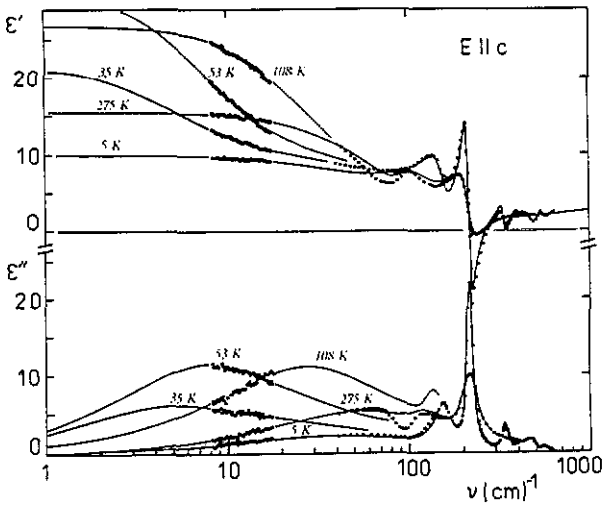

Figure 3. ε_{33} dielectric spectra for several temperatures: ●, experiment; ——, fit (see text). Note the logarithmic frequency scale.

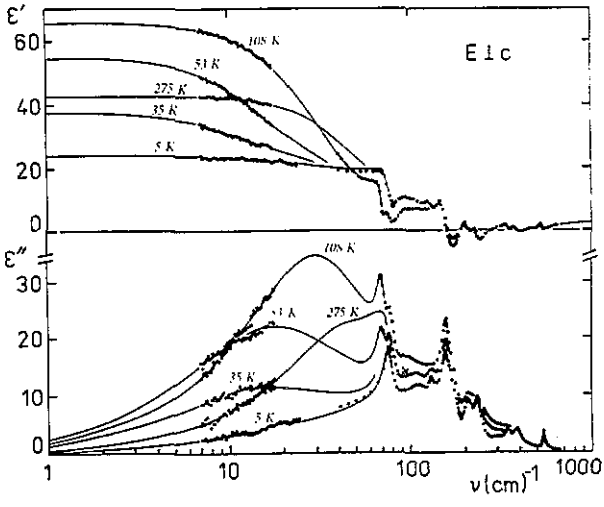

Figure 4. ε_{11} dielectric spectra for several temperatures: ●, experiment; ——, fit (see text). Note the logarithmic frequency scale.

constant. In figures 3 and 4 are shown the selected calculated dielectric spectra on a logarithmic scale for $\boldsymbol{E} \parallel \boldsymbol{c}$ and $\boldsymbol{E} \perp \boldsymbol{c}$ polarization, respectively.

The dielectric spectra $\varepsilon'(\nu)$ and $\varepsilon''(\nu)$ have been fitted by a sum of classical damped oscillators; see the full curves in figures 3 and 4. This fit, although incompletely accurate owing to the neglect of mode coupling, reveals, in our opinion, the main features of the dielectric spectra in the measured spectral range. It should be noted that some of the minor spectral features in figures 1 and 2 above about 300 cm^{-1} might be due to the leakage of improper polarization because of the limited polarization degree of our polarizer in this spectral range. Therefore in our paper we do not pretend to evaluate accurately all phonon parameters as a function of temperature and their detailed assignment. Nevertheless, from the results of our fit, several conclusions can be drawn. Except for the two lowest B_2 modes below 100 and near 130 cm^{-1} at room temperature, all other mode frequencies are almost temperature independent. Also the mode dampings and strengths show only a slight temperature dependence down to the T_g typical of pure

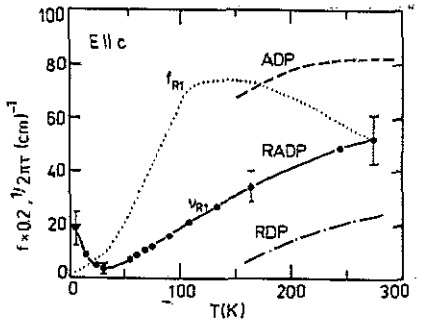

Figure 5. Temperature dependence of the soft 'ferroelectric' relaxation parameters in RADP compared with the behaviour of the both pure compounds.

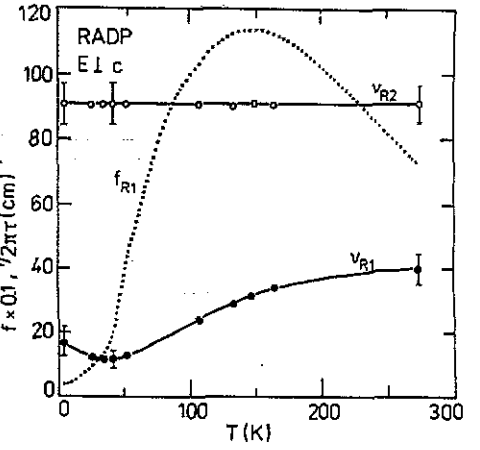

Figure 6. Temperature dependences of both relaxations in $E \perp c$ spectra. The lower-frequency R_1 relaxation represents the 'antiferroelectric' proton-hopping mode; the temperature-independent higher-frequency relaxation R_2 represents a combination of extremely broad O—H vibrations with one-phonon density of state induced by disorder due to breaking of the quasi-momentum selection rule.

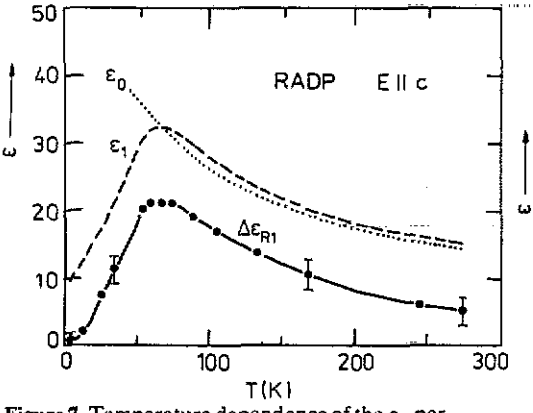

Figure 7. Temperature dependence of the ε_{33} permittivity from our fit at 1 cm^{-1} (ε_1) compared with the low-frequency permittivity ε_0 (Schmidt *et al* 1990). The contribution $\Delta\varepsilon_{R_1}$ of the 'ferroelectric' relaxation is shown separately.

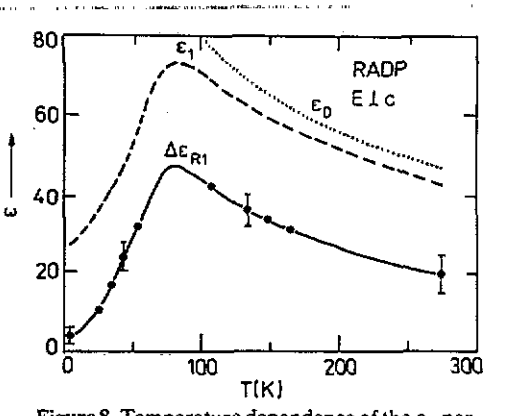

Figure 8. Temperature dependence of the ε_{11} permittivity from our fit at 1 cm^{-1} (ε_1) compared with the low-frequency permittivity ε_0 (Iida and Terauchi 1983). The contribution $\Delta\varepsilon_{R_1}$ of the 'antiferroelectric' relaxation is shown separately.

compounds (Simon *et al* 1988). However, to achieve a good fit, an additional overdamped oscillator was added to all spectra, which accounts for some background absorption. In our fit this background was chosen to be temperature independent (for $E \parallel c$; $\nu_B = 75$ cm^{-1}, the damping $\Gamma_B = 180$ cm^{-1} and the dielectric strength $\Delta\varepsilon_{R_2} = 2.8$; for $E \perp c$ $\nu_B = 165$ cm^{-1}, $\Gamma_B = 300$ cm^{-1} and $\Delta\varepsilon_{R_2} = 15.0$). Whereas for the $E \parallel c$ polarization this background is weak and overlaps with the lowest-frequency soft-mode relaxation above the glass transition, in the case of the $E \perp c$ polarization the background is much stronger and situated in the higher-frequency range.

The parameters of the lowest relaxation R_1 (overdamped oscillator) which are reminiscent of the ferroelectric soft mode and antiferroelectric proton polar mode in the case of RDP ($E \parallel c$ polarization), and ADP ($E \perp c$ polarization), respectively, are shown in figures 5 and 6. In the $E \parallel c$ case, the relaxation frequency ν_{R_1} is compared with the corresponding frequencies for pure ADP and RDP (Volkov *et al* 1980). Note that the relaxation strength $f_{R_1} = \nu_{R_1} \Delta\varepsilon_{R_1}$ (where $\Delta\varepsilon_{R_1}$ is the dielectric contribution of the relaxation R_1) strongly decreases below about 100 K for both polarizations. On the other hand, as already mentioned, the strength f_{R_2} of the 'background' relaxation is temperature independent (about 1350 cm^{-1}) as well as its frequency $\nu_{R_2} = \nu_B^2/\Gamma_B$.

In figures 7 and 8 we compare the dielectric contribution $\Delta\varepsilon_{R_1}$ with the total static permittivity ε_1 from our fit and with the measured low-frequency permittivity ε_0^c (Iida and Terauchi 1983) and ε_0^a (Schmidt *et al* 1990), respectively. One can see that above the glass transition the relaxation R_1 accounts for the whole dielectric anomaly and almost no dispersion occurs in the microwave and lower-frequency range. This is, however, not true below the glass transition as will be discussed in the next section.

4. Discussion

Let us first discuss the behaviour above the glass transition $T_g \simeq 100$ K. Here the spectra are essentially similar to those of pure compounds (Simon *et al* 1988, Wyncke *et al* 1990). In agreement with Raman measurements (Courtens and Vogt 1985, Lee and Kim 1988) and as in the KADP system (Wyncke *et al* 1990), the two B_2 modes near 130 and 220 cm^{-1} (see figure 3) can be assigned to Rb^+–$H_2PO_4^-$ and NH_4^+–$H_2PO_4^-$ translations along the c axis, respectively. This represents a clear case of two-mode behaviour in a mixed-crystal system (see, e.g., Taylor 1988; see also Lee and Kim 1988), which is expected because of the large mass difference between Rb^+ and NH_4^+ ions. The anomalous temperature dependence of the lower mode below T_g is probably connected with a weak appearance of the PO_4 libration in this spectral range (Courtens and Vogt 1985). On the other hand, the broad low-frequency anomalous modes in both B_2 and E spectra which represent mainly the collective proton motion (see, e.g., Simon *et al* 1988) show clearly one-mode behaviour (see figures 5 and 6), again in agreement with Raman data and in analogy to the KADP system (Wyncke *et al* 1990).

Concerning the assignment of the remaining phonon modes, group theory in the paraelectric phase predicts that no other external mode is active for $E \parallel c$ (B_2 modes) whereas seven external modes are expected in $E \perp c$ spectra (E modes) (see, e.g., Courtens and Vogt 1985). External modes consist of $Rb^+(NH_4^+)$–$H_2PO_4^-$ translations and $H_2PO_4^-$ and NH_4 librations and are expected to lie below about 400 cm^{-1}. In particular, the mode near 330 cm^{-1} seen in both polarizations at lower temperatures can be assigned to NH_4^+ librations (Courtens and Vogt 1985). Its clear appearance in the B_2 spectra where it is forbidden in the paraelectric phase gives evidence of strong local polar distortions, at least below T_g. It should be noted that the temperature dependence of this mode is similar to that seen in Raman E spectra (Courtens and Vogt 1985) (except for a somewhat higher frequency in our case) where it is allowed in the paraelectric phase. The anomalous temperature dependence was assigned to strengthening of the bonding between ammonia and surrounding oxygen atoms below T_g (Courtens and Vogt 1985).

The remaining external E modes lie below 300 cm^{-1} and it is difficult to assign them in detail. The higher-frequency modes belong to internal ν_2 (around 400 cm^{-1}) and ν_4

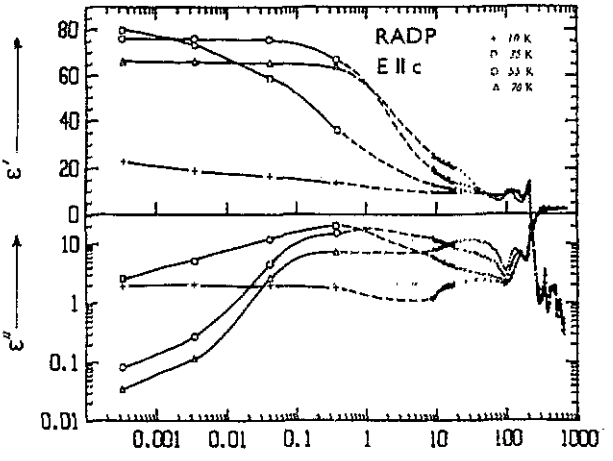

Figure 9. Broad-range ε_{33} dielectric spectra for RADP below T_g. The data below 1 cm^{-1} are taken from Brückner *et al* (1988). The full, broken and dotted curves are guides for the eye.

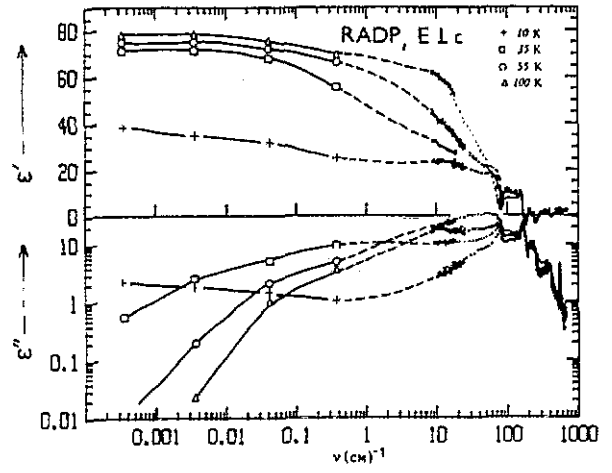

Figure 10. Broad range ε_{11} dielectric spectra for RADP below T_g. The data below 1 cm^{-1} are taken from Brückner *et al* (1988). The full, broken and dotted curves are guides for the eye.

(above 500 cm^{-1}) PO_4 vibration. They do not show any dramatic temperature changes and will not be further discussed.

The pronounced absorption background in the $E \perp c$ spectra was observed also in the case of pure RDP above T_c and was assigned to the low-frequency wings of extremely broad proton stretching modes (Simon *et al* 1988). The same assignment can be used in our case. In the case of pure compounds this background disappears with proton ordering below T_c. However, in the case of glassy mixed crystals it survives also below T_g down to the lowest temperatures. In this case its origin is probably connected also with disorder-induced one-phonon absorption due to the breaking of the quasi-momentum conservation selection rule (see, e.g., Barker and Sievers 1975). This mechanism is operative even if the disorder is frozen in as in canonical glasses.

Finally, let us discuss the most interesting phenomenon in dipolar glasses, namely the behaviour of low-frequency losses below T_g. The difference between the measured low-frequency permittivity ε_0 and submillimetre permittivity ε_1 below about T_g clearly indicates additional dielectric dispersion not accounted for by our fit. In fact, previous audiofrequency (Courtens 1984, 1986) and microwave dielectric measurements (Brückner *et al* 1988) revealed this dispersion for the $x = 0.35$ RADP system. In figures 9 and 10

we tried to compare the microwave and our submillimetre data in a broad logarithmic scale. Even though the data have been obtained on samples with different NH_4 concentrations ($x = 0.34$ and $x = 0.5$, respectively) one can see that the two data sets nearly merge in the non-investigated interval 0.3–8 cm^{-1}. Visual inspection of the low-temperature spectra shows that the spectral part below about 50 cm^{-1} consists of two overlapping dispersion regions: the higher-frequency region which was considered in our fit and the lower-frequency region which broadens at the low-frequency end far beyond the scale of figures 9 and 10 on cooling below about 50 K.

The origin of the higher-frequency submillimetre mode is probably the same as in pure compounds; it consists basically of collective acid proton hopping which obeys the ice rules, i.e. preserves the configuration of two protons near each PO_4^{3-} group, coupled to other polar phonon modes (Simon *et al* 1988). The origin of the broad lower-frequency dispersion was suggested by Schmidt (1988a, b) to be due to the diffusion of thermally activated HPO_4^{2-} and H_3PO_4 Takagi defects, which in fact represents another collective proton-hopping mechanism (Popova and Bystrov 1987). To confirm quantitatively this theory, one needs to separate contributions from both types of dispersion process. This seems to be an ambiguous procedure owing to the strong overlap of both processes. Easier separation of both processes seems to be possible in deuterated DRADP or DRADA glass systems, where audiofrequency dielectric measurements (Courtens 1986, Kutnjak *et al* 1990) revealed clear loss maxima as a function of frequency. Infrared and near-millimetre measurements are in progress on such systems to obtain the full dielectric spectrum which is easier to interpret than in the case of undeuterated salts.

References

Barker A S Jr and Sievers A J 1975 *Rev. Mod. Phys.* Suppl. 2 **47** 1
Binder K and Young A P 1986 *Rev. Mod. Phys.* **58** 801
Brückner H J, Courtens E and Unruh H G 1988 *Z. Phys.* B **73** 337
Courtens E 1984 *Phys. Rev. Lett.* **52** 69
—— 1986 *Phys. Rev.* B **33** 2975
—— 1987 *Ferroelectrics* **72** 229
Courtens E and Vacher R 1987 *Phys. Rev.* B **35** 7271
Courtens E and Vogt H 1985 *J. Chim. Physique* **82** 317
—— 1986 *Z. Phys.* B **62** 143
Courtens E, Huard F and Vacher R 1985 *Phys. Rev. Lett.* **55** 722
Courtens E, Vacher R and Dagorn Y 1986 *Phys. Rev.* B **33** 7625
Iida S and Terauchi H 1983 *J. Phys. Soc. Japan* **52** 4044
Kutnjak Z, Levstik A, Filipič C, Kabelka H, Fuith A and Warhanek H 1991 *Phys. Rev.* B at press
Le Calve N, Romain F, Limage M H and Novak A 1989 *J. Mol. Struct.* **200** 131
Lee K S and Kim J J 1988 *J. Phys. Soc. Japan* **57** 3270
Popova E A and Bystrov D S 1987 *Ferroelectrics* **72** 45
Schmidt V H 1988a *Ferroelectrics* **78** 207
—— 1988b *J. Mol. Struct.* **177** 257
Schmidt V H, Trybula Z, He D, Drumheller J E, Stigers C, Li Z and Howell F L 1990 *Ferroelectrics* **106** 119
Simon P, Gervais F and Courtens E 1988 *Phys. Rev.* B **37** 1969
Taylor D W 1988 *Optical Properties of Mixed Crystals (Modern Problems in Condensed Matter Science 23)* ed R J Elliott and I P Ipatova (Amsterdam: North-Holland) p 35
Volkov A A, Goncharov Yu G, Kozlov G V, Lebedev S P and Prokhorov A M 1985 *Infrared Phys.* **25** 369
Volkov A A, Kozlov G V, Lebedev S P, Prokhorov A M 1980 *Ferroelectrics* **25** 531
Wyncke B, Brehat F and Vaezzadeh M 1990 *Ferroelectrics* **107** 139